

HNPS Advances in Nuclear Physics

Vol 27 (2019)

HNPS2019



Measurement of differential cross sections of deuteron elastic scattering on ^{31}P for EBS purposes

Natalia Bligoura, Eleni Ntemou, Xenophon Aslanoglou, Michael - Kokkoris, Anastasios Lagoyannis, Fotis Maragkos, Panagiotis Misaelides, Nikolaos Patronis, Kostas Preketes-Sigalas

doi: [10.12681/hnps.2999](https://doi.org/10.12681/hnps.2999)

To cite this article:

Bligoura, N., Ntemou, E., Aslanoglou, X., Kokkoris, M. .-, Lagoyannis, A., Maragkos, F., Misaelides, P., Patronis, N., & Preketes-Sigalas, K. (2020). Measurement of differential cross sections of deuteron elastic scattering on ^{31}P for EBS purposes. *HNPS Advances in Nuclear Physics*, 27, 131–137. <https://doi.org/10.12681/hnps.2999>

Measurement of differential cross sections of deuteron elastic scattering on ^{31}P for EBS purposes

N. Bligoura¹, E. Ntemou^{1,2}, X. Aslanoglou³, M. Kokkoris¹, A. Lagoyannis²,
F. Maragos¹, P. Misaelides⁴, N. Patronis³, K. Preketes–Sigalas^{1,2}

¹ Department of Physics, National Technical University of Athens, Zografou Campus, 15780 Athens, Greece

² Tandem Accelerator Laboratory, Institute of Nuclear Physics, N.C.S.R. “Demokritos”, Aghia Paraskevi, 15310 Athens, Greece

³ Department of Physics, University of Ioannina, 45110 Ioannina, Greece

⁴ Department of Chemistry, Aristotle University, GR-54124 Thessaloniki, Greece

Abstract The $^{31}\text{P}(d,d_0)^{31}\text{P}$ elastic scattering differential cross-sections were measured, for the first time, in the energy range $E_{d,\text{lab}}=900\text{--}2400\text{ keV}$, using a variable energy step, for elastic backscattering spectrometry (EBS) purposes. The measurements were performed at the 5.5 MV TN11 HV Tandem Accelerator of the N.C.S.R. “Demokritos”, implementing a high precision goniometer. The experimental setup consisted of five silicon surface barrier (SSB) detectors, placed at the laboratory scattering angles between 130° and 170° (in steps of 10°). The target used was a thin GaP layer evaporated on a self-supporting carbon foil. To validate the obtained results, benchmarking measurements were performed, using a polished GaP crystal. The determined cross-section datasets are compared with the corresponding ones using Rutherford’s formula, and similarities and discrepancies will be discussed and analyzed.

Keywords Differential cross sections, d–EBS, IBA

Corresponding author: N. Bligoura (phnatalia69@gmail.com) | Published online: May 1st, 2020

INTRODUCTION

Phosphorus, with ^{31}P being the only stable isotope, is a light chemical element and essential to all living organisms. However, it is highly reactive, therefore it is never found as a free element in nature but in various forms of compounds. The majority of phosphorus compounds are used in fertilizers. Nevertheless, due to the high mobility of phosphorus, the widespread use of fertilizers leads to the risk of P infiltrating to surface waters where it may promote eutrophication [1]. Therefore, over the past few years, environmental and agronomic studies have been significantly enhanced in order to acquire knowledge about the depth concentration of phosphorus in soils. Moreover, phosphorus is an important ingredient in steel production. It is used as an alloying element in copper with oxygen to increase the hydrogen embrittlement resistance compared to normal copper and it is additionally added in interstitial free steels (IF steels) in order to improve solidification resulting in the increment of their resistance [2]. Furthermore, phosphorus finds multiple utilizations in the field of the semiconductor industry, namely in integrated circuits, where, as a constituent in borophosphosilicate glass (BPSG), it is used for interlevel dielectrics [3]. It is also added in SiC devices to enhance their electrical quality [4]. Thus, the precise quantitative determination of phosphorus depth profile concentrations is essential for several applications and particularly in semiconductor structures, as phosphorus presents anomalous diffusion phenomena [5].

To achieve this goal, the SIMS (Secondary Ion Mass Spectrometry) technique is frequently performed for the determination of the depth distribution of phosphorus, although quantification is usually not possible if it is not combined with another technique [6]. Furthermore, several other IBA

(Ion Beam Analysis) techniques can produce accurate quantitative phosphorus depth profile concentrations, specifically ERDA (Elastic Recoil Detection Analysis) for thin, surficial layers, p-EBS (Elastic Backscattering Spectroscopy) due to the existence of evaluated and benchmarked differential cross-section datasets in literature and NRA (Nuclear Reaction Analysis). Actually, as apparent in literature, the combination of more than one techniques is usually preferable [4,6]. Amongst the previously introduced IBA techniques the most commonly used one is NRA, especially via the reactions $^{31}\text{P}(\text{a},\text{p}_0)^{34}\text{S}$ and $^{31}\text{P}(\text{p},\text{a}_0)^{28}\text{Si}$ [6,7]. The main disadvantage in the implementation of these reactions is that the Q-values involved are rather poor (0.627 MeV and 1.916 MeV respectively). On the other hand, the deuteron induced NRA (d-NRA) appears to be the most promising technique for phosphorus depth profiling in complex matrices, since it produces isolated high energy peaks with practically no background, since the Q-values involved are 5.711 MeV for the $^{31}\text{P}(\text{d},\text{p}_0)^{32}\text{P}$ and 8.165 MeV for the $^{31}\text{P}(\text{d},\text{a}_0)^{29}\text{Si}$ reaction. Nevertheless, d-NRA's full implementation, implying the combination with the Elastic Scattering Spectrometry (EBS) technique, is usually prevented by the significant lack of the associated d-EBS differential cross-section datasets in literature.

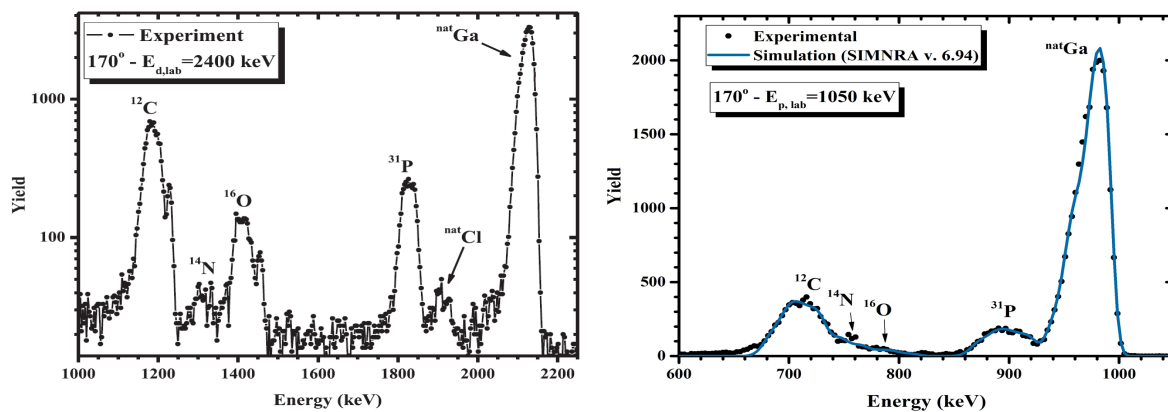


Figure 1. (left) The experimental deuteron spectrum of the thin GaP layer evaporated on top of a self-supported carbon foil taken at $E_{d,\text{lab}} = 2400$ keV and 170° (right) The experimental and simulated, using the SIMNRA code, proton spectra obtained at $E_{p,\text{lab}} = 1050$ keV and 170° , along with the corresponding peak identification.

To address this problem, the differential cross sections of deuteron elastic scattering on ^{31}P were determined, in the present work for the first time, for the deuteron energy range $E_{d,\text{lab}} = 900\text{--}2400$ keV (in energy steps of $\sim 10\text{--}30$ keV) and for the detection angles of $130^\circ\text{--}170^\circ$ with steps of 10° , suitable for analytical purposes. The results of the present work are already available to the scientific community via IBANDL (www-nds.iaea.org/ibandl/) in both graphical and tabular forms.

EXPERIMENTAL SETUP

Two different sets of measurements were implemented, one for the determination of the differential cross section values and subsequently one for their validation (benchmarking). Both of these sets of measurements were conducted at the 5.5 MV TN11 HV Tandem Accelerator of N.C.S.R. “Demokritos”, Athens, Greece. Experimental aspects concerning the goniometer, the determination of the final beam energy, the detection system, and the electronics can be found in the publication of the deuteron elastic scattering on sodium, $^{23}\text{Na}(\text{d},\text{d}_0)^{23}\text{Na}$, by Ntemou et al. [8] as both experiments proceeded simultaneously and shared the same experimental setup and detection system.

The target used during the experiment was a thin GaP layer, which was manufactured at the Tandem Laboratory of N.C.S.R. “Demokritos” by evaporating high-purity GaP powder on top of a

thin C stripping foil, with the Ga presence needed for normalization purposes. A typical spectrum presented in Fig. 1 (left) for the highest deuteron energy at 2400 keV at a scattering angle of 170°. It should be noted that minor contributions of nitrogen and chlorine are evident in the spectrum due to the coating used for the manufacture of self-supporting carbon foils, while the oxygen contribution is originating from the evaporation procedure itself. For the validation of the obtained cross-section values the target used was a GaP polished crystal, which was bombarded with deuterons at energies 1110, 1320, 1500, 1640, 1820, 2060 and 2300 keV, and the backscattered beam particles were detected by five detectors set at the scattering angles of 130°, 140°, 150°, 160° and 170°.

The estimation of the mean deuteron beam energy at half of the target's thickness, the energy loss, the energy straggling, as well as the characterization of the target were carried out using the SIMNRA (v. 6.94) code [9], as described in [8].

RESULTS AND DATA ANALYSIS

The determination of the differential cross-section values $d\sigma/d\Omega$ for ^{31}P was carried out using the relative measurement technique, as described in [8], via the corresponding formula:

$$\left(\frac{d\sigma}{d\Omega}\right)_{\theta,E,P} = \left(\frac{d\sigma}{d\Omega}\right)_{\theta,E,Ga} \times \frac{Y_P}{Y_{Ga}} \times \frac{N_{Ga}}{N_P}$$

where θ is the scattering angle, E the energy at the half of the target's thickness (following the accelerator energy calibration), Y_P and Y_{Ga} are the experimental yields, and N_{Ga}/N_P is the ratio of the atomic areal density of Ga to the atomic areal density of P within the GaP layer present in the target.

The first term, $\left(\frac{d\sigma}{d\Omega}\right)_{\theta,E,Ga}$, indicates the deuteron Rutherford cross-section values from Ga at the energy E and scattering angle θ (in the energy region of the present experiment the backscattering of deuterons from Ga is purely Rutherford). The electron screening effect was also estimated using L'Ecuyer's correction factor. [10].

The experimental yields were determined either by integrating or by fitting the experimental spectra following the background subtraction, using the code Tv [11]. Although the integration technique is ordinarily preferable, at certain scattering angle–beam energy combinations, where the gallium and the phosphorus peaks partially overlapped, the fitting procedure was considered necessary. Notwithstanding, the statistical uncertainty did not exceed 2.5% in all cases.

The thickness ratio Ga:P was determined using the same experimental setup and the proton spectra obtained, for this purpose, at energies 1050, 1100, 1200, 1360, 1430 keV for the scattering angles of 150°, 160°, and 170°. Due to the structure of the $^{31}\text{P}(p,p_0)^{31}\text{P}$ cross section and to maximize the accuracy of the target thickness calculation, the proton beam energies were chosen far from the existing Breit–Wigner type resonances. The process of calculating the target thickness with SIMNRA was initiated by keeping the Ga thickness constant for all the beam energy/scattering angle combinations and fitting the product $Q \times \Omega$ on the gallium peak using the Rutherford cross-section datasets. By repeating this procedure, the total P areal density (in atoms/cm²) was determined for every proton beam/scattering angle combination, by slightly varying the phosphorus composition in each case. The simulation of the phosphorus peak was achieved using non–Rutherford evaluated datasets [12], as received from the online calculator SigmaCalc 2.0, which has also been recently benchmarked [13]. It should be remarked here that for the scattering angle of 150°, only two beam energies were used (1430, 1360 keV), since for lower beam energies a partial overlap between the gallium and phosphorus peaks existed. A typical spectrum is presented in Fig. 1 (right) for the proton energy 1050 keV and the scattering angle of 170° along with the simulation results. The average value of the target thickness was estimated to be 2.00 ± 0.08 , indicating a 4% relative statistical uncertainty. This statistical uncertainty does not include, however, any systematic uncertainties, specifically due to

the implemented stopping power compilations, and to possible lateral inhomogeneities in the target composition. In the SRIM website, there is no existing data concerning deviations between compiled and experimental stopping power data neither for the case of phosphorus nor for gallium. However, discrepancies could be observed by testing neighbouring nuclei, for both elements. For the phosphorus case, namely silicon, shows differences up to 4% and for the gallium case the neighbouring nuclei, namely germanium and zinc, display differences between 1.4% to 4.4%.

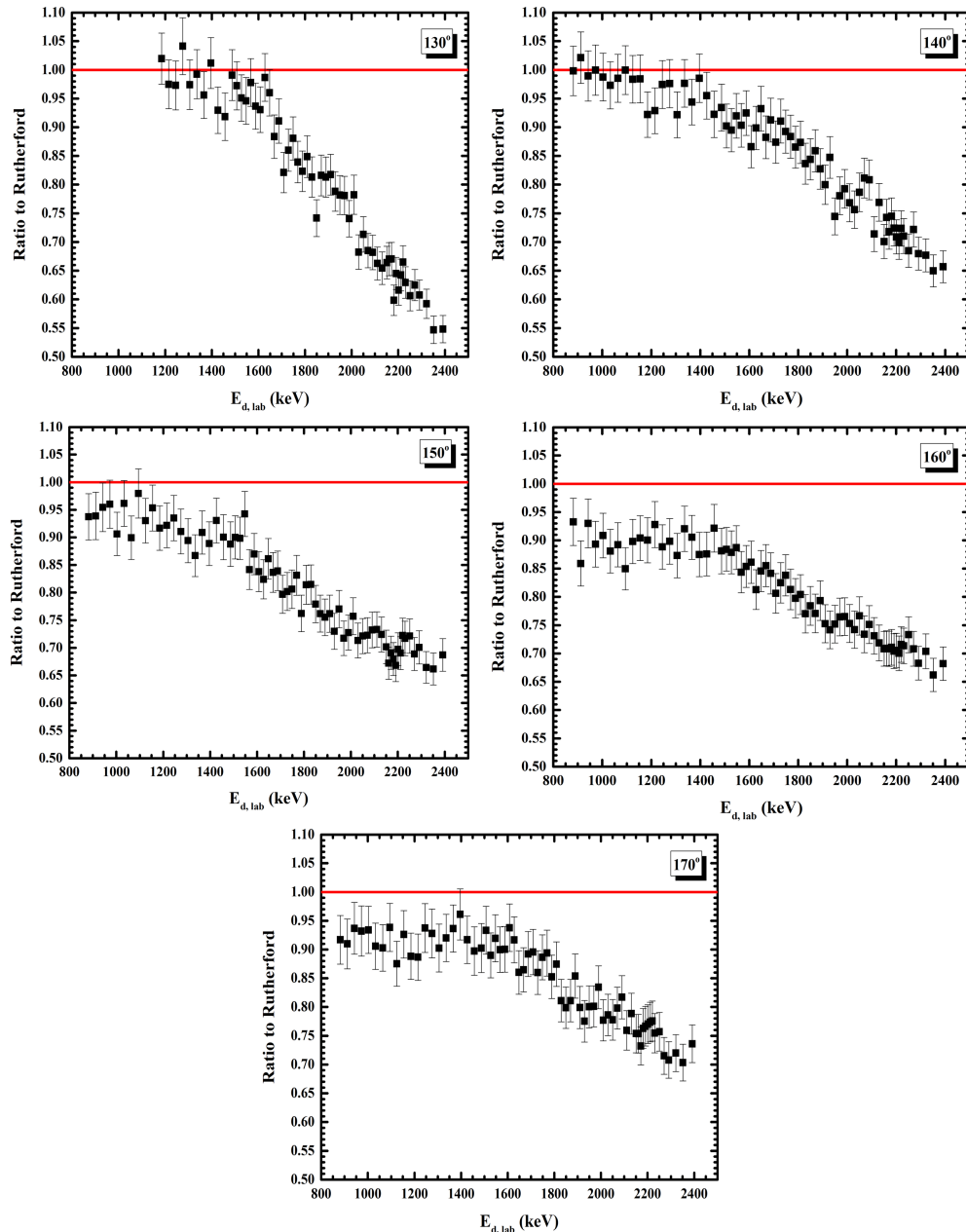


Figure 2. The ratio of the obtained differential cross-section values for the deuteron elastic scattering on ^{31}P to the calculated ones using Rutherford's formula, for $E_{d,\text{lab}} = 900\text{--}2400$ keV in energy steps of 10–30 keV and for the five backscattering angles of 130° , 140° , 150° , 160° , 170° . The total evaluated statistical uncertainties are included in the graphs; in the x-axis, the uncertainties are not noticeable due to the selected scale.

DISCUSSION AND BENCHMARKING

The ratios to Rutherford of the obtained differential cross-section values for the deuteron elastic

scattering on ^{31}P for five backscattering angles (130° , 140° , 150° , 160° , 170°) are presented in graphical form (Fig. 2). The total statistical experimental uncertainty, excluding the systematic uncertainties introduced by the parameters mentioned above, did not exceed $\sim 5\%$ in all cases. The experimental results indicate deviations from the corresponding Rutherford ones over almost the whole energy range under study and in some cases are up to $\sim 45\%$. This is unexpected, particularly, since, the only values that are equal, within error, with the Rutherford ones correspond to low energies at the most forward angles (130° , 140°). At all angles, a notable drop is observed at higher energies. A surprising result is revealed for low energies at the most backward angles (150° , 160° , 170°), where the obtained cross-section values were lower than the corresponding Rutherford ones. The deuteron elastic scattering on phosphorus is expected to be nearly pure Coulomb for lower energies, as seen for the deuteron elastic scattering on silicon [14]. The correlation between the ^{31}P and ^{28}Si was selected due to the close Q -values for deuteron capture and the similar Coulomb barriers, although ^{31}P is an odd-even nucleus. Additional investigation is needed regarding this phenomenon over a variety of similar beam–target combinations before a firm conclusion is reached. The available spectroscopic data indicate the existence of a level of the compound nucleus ^{33}Si with energy $E_{x^*} = 17.360$ keV and $\Gamma = 58$ keV, which should be observed at $E_{d,\text{lab}} = 2213$ keV. Even though a more dense energy step was chosen in the present work (10 keV) near this value, the experimental results did not show a resonant type of behavior. Moreover, as illustrated in Fig. 3, the angular variation was rather smooth.

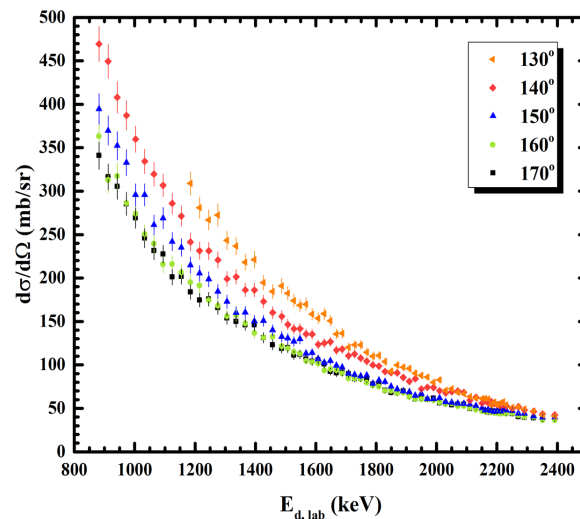


Figure 3. The differential cross-section values (mb/sr) for the $^{31}\text{P}(d,d_0)^{31}\text{P}$ elastic scattering for all backscattering angles, measured at $E_{d,\text{lab}} = 900\text{--}2400$ keV.

To validate the results deuteron elastic scattering benchmarking spectra were obtained from a GaP polished crystal at several energies over the whole energy range under study, and more specifically at energies 1110, 1320, 1500, 1640, 1820, 2060, 2300 keV and for five scattering angles (130° , 140° , 150° , 160° , 170°). The simulation of the experimental spectra was achieved using the SIMNRA program with Rutherford cross-section datasets, including screening effects, for the gallium deuteron elastic edge (i.e. for both stable gallium isotopes, ^{69}Ga and ^{71}Ga) and the differential cross-section datasets defined in the present work for the deuteron elastic scattering on phosphorus. Nevertheless, no benchmarking results were analyzed for the deuteron energies 1320, 2060 and 2300 keV, due to the existence of significant channeling perturbations near the surface, despite the precise positioning of the thick crystalline target. Consequently, the benchmarked results refer only to the remaining energies (1110, 1500, 1640, 1820 keV). Four of them are presented (Fig. 4), along with the collected

simulated ones for different deuteron beam-scattering angle combinations (specifically at 1110 keV – 140°, 1500 keV – 170°, 1640 keV – 160° and 1820 keV – 150°) and the corresponding edge identification. The correlation between the experimental and the simulated spectra was accomplished over an energy window of ~200 keV (~65 channels) below the phosphorus edge, where the number of the simulated and experimental counts were compared and the differences were within ~7%. The integrated window was meticulously selected in order for the energy straggling and the plural scattering to be less important and is denoted in Fig. 4 with a dashed blue line.

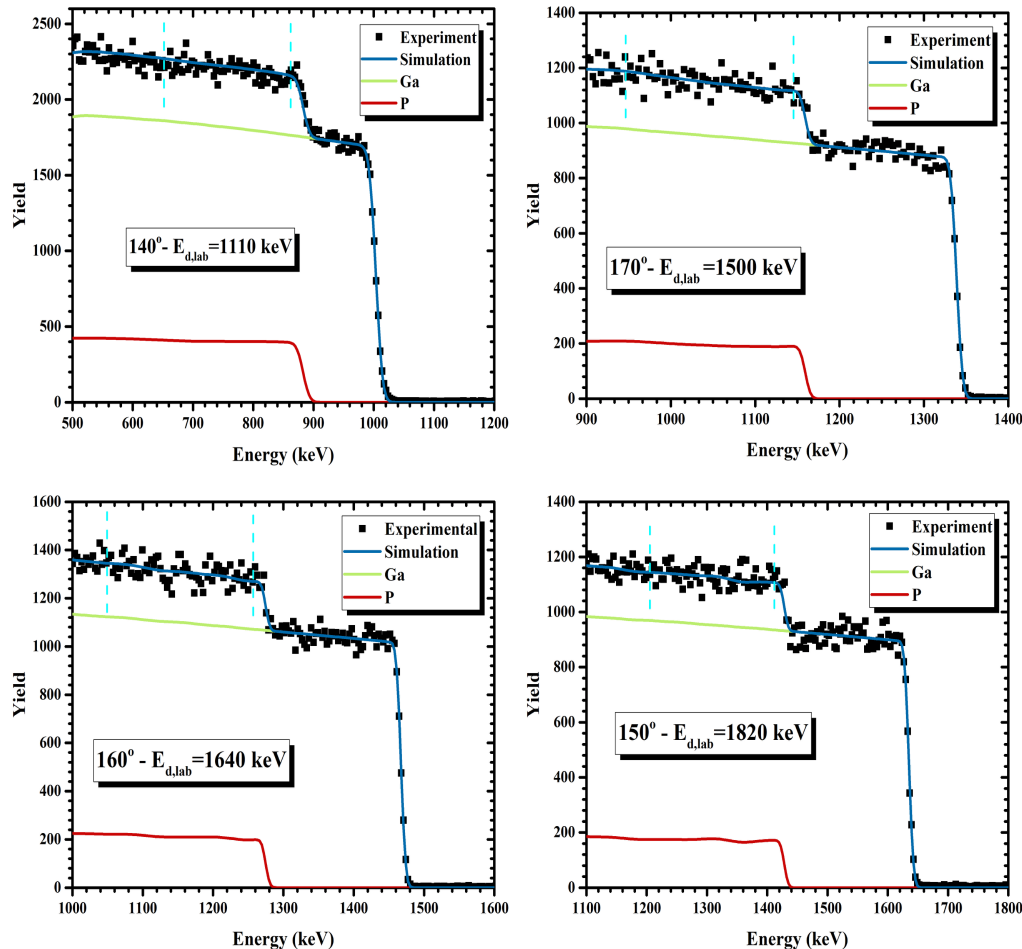


Figure 4. The typical experimental and simulated, using the SIMNRA code, spectra of the thick target (GaP) at different beam energy and scattering angle combinations along with the corresponding edge identification. As signified in the graphs by dashed lines, the energy window used in the benchmarking procedure was ~200 keV (~65 channels) below the phosphorus surface edge, depending on the beam energy.

SUMMARY AND CONCLUSIONS

The differential cross-section values measured, for the first time, for the deuteron elastic scattering on phosphorus for the deuteron energy range 900–2400 keV with a variable energy step (10–30 keV), depending on the available spectroscopic information, and for the backscattering angles of 130°–170° with a 10° step. The results of this work revealed small deviations from the Rutherford formula at low deuteron beam energies and higher deviations at high energies, in some cases up to 45%, along with a smooth angular variation. The obtained differential cross-section datasets were subsequently validated by irradiating a polished GaP crystal target. The results unveiled a very good

agreement with the experimental spectra (better than $\sim 7\%$). Hence, these results are considered suitable for analytical purposes through the simultaneous implementation of the d-EBS technique, along with the d-NRA one, for the coherent determination of phosphorus depth profile concentrations.

Acknowledgments

This research is co-financed by Greece and the European Union (European Social Fund-ESF) through the Operational Programme «Human Resources Development, Education and Lifelong Learning» in the context of the project “Strengthening Human Resources Research Potential via Doctorate Research” (MIS-5000432), implemented by the State Scholarships Foundation (IKY). The authors would like to acknowledge the support of this work by the project “CALIBRA/EYIE” (MIS 5002799) which is implemented under the Action “Reinforcement of the Research and Innovation Infrastructure”, funded by the Operational Programme “Competitiveness, Entrepreneurship and Innovation” (NSRF 2014-2020) and cofinanced by Greece and the European Union (European Regional Development Fund).

References

- [1] A.K. Eriksson et al., *Geoderma* 280, 29 (2016)
- [2] A.P. da Rocha Santos et al., *J. Mat. Res. Tech.* 7, 331 (2018)
- [3] D.S. Walsh et al., *Nucl. Instr. Meth. Phys. Res. B* 161-163, 629 (2000)
- [4] E. Pitthan et al., *Nucl. Instr. Meth. Phys. Res. B* 371, 220 (2016)
- [5] A.M. Mironov et al., *Vacuum* 83, S127 (2009)
- [6] M.A. Bolorizadeh et al., *Nucl. Instr. Meth. Phys. Res. B* 225, 354 (2004)
- [7] S. Ferdjani et al. *J. All. Comp.* 200, 191 (1993)
- [8] E. Ntemou et al., *Nucl. Instr. Meth. Phys. Res. B* 461, 124 (2019)
- [9] M. Mayer, *Nucl. Instr. Meth. Phys. Res. B* 332, 176 (2014)
- [10] J. L’Ecuyer, et al., *Nucl. Instr. Meth. Phys. Res. B* 160, 337 (1979)
- [11] J. Theuerkauf et al., Institute of Nuclear Physics, “Program tv”, Cologne (1993, unpublished)
- [12] A.F. Gurbich et al., *Nucl. Instr. Meth. Phys. Res. B* 268, 1703 (2010)
- [13] V. Paneta et al., *Nucl. Instr. Meth. Phys. Res. B* 328, 1 (2014)
- [14] E. Ntemou et al., *Nucl. Instr. Meth. Phys. Res. B* 450, 24 (2019)